

Article

Electrical Impedance Spectroscopy for Detection of Cells in Suspensions Using Microfluidic Device with Integrated Microneedles

Muhammad Asraf Mansor ¹, Masaru Takeuchi ², Masahiro Nakajima ², Yasuhisa Hasegawa ² and Mohd Ridzuan Ahmad ^{3,*}

¹ Faculty of Biosciences and Medical Engineering, Universiti Teknologi Malaysia, Skudai 81310, Johor, Malaysia; asraf@biomedical.utm.my

² Department of Micro-Nano Systems Engineering, Nagoya University, Nagoya 464-8603, Japan; takeuchi@mein.nagoya-u.ac.jp (M.T.); nakajima@mein.nagoya-u.ac.jp (M.N.); hasegawa@mein.nagoya-u.ac.jp (Y.H.)

³ Faculty of Electrical Engineering, Universiti Teknologi Malaysia, Skudai 81310, Johor, Malaysia

* Correspondence: mdridzuan@utm.my; Tel.: +60-13-7612-778; Fax: +60-7-5566-272

Academic Editor: Fan-Gang Tseng

Received: 21 December 2016; Accepted: 5 February 2017; Published: 11 February 2017

Abstract: In this study, we introduce novel method of flow cytometry for cell detection based on impedance measurements. The state of the art method for impedance flow cytometry detection utilizes an embedded electrode in the microfluidic to perform measurement of electrical impedance of the presence of cells at the sensing area. Nonetheless, this method requires an expensive and complicated electrode fabrication process. Furthermore, reuse of the fabricated electrode also requires an intensive and tedious cleaning process. Due to that, we present a microfluidic device with integrated microneedles. The two microneedles are placed at the half height of the microchannel for cell detection and electrical measurement. A commercially-available Tungsten needle was utilized for the microneedles. The microneedles are easily removed from the disposable PDMS (Polydimethylsiloxane) microchannel and can be reused with a simple cleaning process, such as washing by ultrasonic cleaning. Although this device was low cost, it preserves the core functionality of the sensor, which is capable of detecting passing cells at the sensing area. Therefore, this device is suitable for low-cost medical and food safety screening and testing process in developing countries.

Keywords: impedance flow cytometry; microneedle; cell concentration detection

1. Introduction

The detection and quantification of cells in complex samples remains a challenge and an important issue for applications such as medical diagnosis and food safety. For medical diagnosis, the detection of cancer cells and pathogenic bacteria cells in the blood is utilized to diagnose disease. The detection of circulating tumor cells (CTCs) in the blood has been shown to be clinically important for early stage metastasis or the recurrence of cancer. The presence of rare CTCs in the blood ranges from only 1 to 100 CTCs/mL blood [1]. *Plasmodium falciparum malaria*—which mainly kills children in developing countries—infests the blood of patients at a concentration of $\sim 1/50$ μL of blood [2]. Regarding food safety, the contamination of drinking water or wastewater with microorganisms such as *E. coli* and *Salmonella* has been a serious issue for several developing countries [3]. As those bacteria can multiply rapidly, it is necessary to detect them quickly, easily, and inexpensively. In order to meet the requirements for these applications, the platforms need to be rapid, sensitive, and cost-efficient.

The classical method for cell detection in suspension is through the use of flow cytometry, which is a rapid and highly accurate measurement technique. This technique—first reported by

Coulter [4]—has emerged in microfabricated devices in order to analyze microscale particles with high sensitivity. For instance, colloids as small as 87 nm could be detected by a microchip Coulter counter on a quartz substrate [5]. However, flow cytometry has high manufacturing cost and involves the labelling of cells with fluorescent antibodies [6]. Recently, impedance flow cytometry (IFC) has gained attention as a significant promising technique to replace and overcome the limitations associated with flow cytometry. IFC is preferable because it is a fast, real-time, and non-invasive method for biological detection. This technique can be utilized in cell counting [7], cancer cell detection [8], and bacteria detection [9]. Some groups have demonstrated detection and counting of cells by using a microfluidic integrated with an electrode for various electrical measurement methods for the applications of food safety [10] and real-time monitoring of bio-threats [11]. This measurement technique is based on the alteration of impedance across measurement electrodes due to the decreasing of ionic current passing between electrodes when a cell is present.

IFC is capable of distinguishing and counting lymphocytes, monocytes, and neutrophils in whole human blood [7]. The concentration of spermatozoa in semen also causes a change in impedance when passing the electrodes [12]. Other studies reported that IFC can detect the presence of cells based on probing the impedance inside the cell at a frequency greater than 1 MHz [13]. A fabricated nanoneedle probe inside a microfluidic was utilized to measure the presence of cells at the sensor surface, making it sensitive to the dielectric properties of solution [14]. However, this device requires patterning of the electrode or probe on the substrate, resulting in higher cost of the fabrication process. Another limitation is the time-consuming cleaning process of the device. Several groups have demonstrated that the technique reduces the cost of microfabrication of electrodes by using printed circuit board (PCB) as a measurement electrode. They demonstrated contactless conductivity detection in a capillary electrophoresis environment [15] and contactless cell manipulation using dielectrophoresis [16]. Recently, contactless impedance cytometry was developed to reduce the fabrication cost of an impedance cytometry device [17,18]. The electrode was fabricated on a PCB substrate (reusable component), and the thin bare dielectric substrate bonded to a PDMS (Polydimethylsiloxane) microchannel (disposable component) was placed onto PCB substrate. The sensitivity of this device is a limitation, since the electric field is buried in a dielectric substrate and does not reach the electrolyte. Several IFC designs and methods have been reported for the detection and analysis of cells [19–21].

In this paper, we propose a novel integrated microneedles-microfluidic system for the detection of yeast cell concentration in suspension and discrimination of the various ionic concentrations of solution (e.g., $1 \times \text{PBS}$, $5 \times \text{PBS}$, and $10 \times \text{PBS}$; PBS: phosphate-buffered saline). The development of the device focuses on reducing the fabrication cost while preserving the main functionality (i.e., cell detection). The significant fabrication cost reduction in this work is achieved by replacing the microfabrication of electrodes with the microneedles. This device utilizes a tungsten needle as a measurement electrode which can be reused and easily cleaned. The two microneedles were placed at half height in a disposable microchannel to detect and enable impedance measurement of passing cells through the applied electric field. Figure 1a illustrates a schematic diagram of the proposed microfluidic chip, which consists of two microneedles integrated at both sides of the microchannel. The main sensing area microchannel length, width, and thickness are 100 μm , 25 μm , and 25 μm , respectively. The device is suitable for early cancer cell detection and water contamination application in developing countries, since it significantly reduces the fabrication cost (i.e., fabrication of the micro electrode is not required).

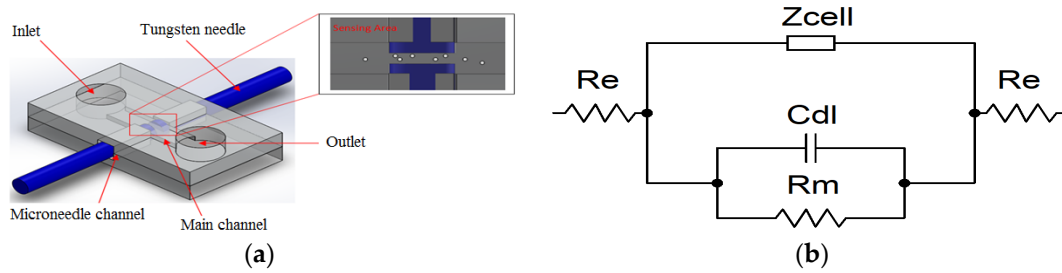


Figure 1. (a) 3D schematic diagram of the device structure and top view of sensing area; (b) An equivalent circuit model of sensing area of microfluidic chip. C_{dl} : capacitance of double layer; R_e : electrode resistance; R_m : solution resistor; Z_{cell} : cell impedance.

2. Principle

The basic principle of detecting suspended biological cells in media is based on Ohm's law. An AC current with a frequency sweep was applied across passing cells to determine the changing impedance value of the media. An equivalent circuit model to understand the interface of two microneedles with the suspension media was developed, as represented in Figure 1b. The sensing area of the microfluidic chip can be modelled electrically as cell impedance Z_{cell} in parallel with the impedance contributed by all materials between the two electrodes, which consist of a solution resistor R_m in parallel with the capacitance of double layer C_{dl} . Both impedance in series with a pair of electrodes resistance R_e . The Z_{cell} represents a cytoplasm resistor (R_c) in series with a membrane capacitor (C_c) [22]. The overall impedance of the measurement system Z_T is given by [23].

$$Z_T = 2R_e + \frac{1}{\frac{1}{R_m} + j\omega C_{dl} + \frac{1}{R_c - j\omega C_c}} \quad (1)$$

where ω is the angular frequency of the electrical signal. As a result, the Z_T changes according to the concentration of suspension medium flow at the sensing area, because of the number of cells present in the medium. Our main focus in the measurement is impedance at the interface of the electrode (microneedle) and electrolyte (solution medium).

3. Experimental

3.1. Cell Culture

In the present study, we used *Saccharomyces cerevisiae* cells as a model for proof of concepts. *Saccharomyces cerevisiae* were cultivated in a petri dish containing 10 mL of YPD broth (Yeast extract Peptone Dextrose). The YPD broth contained 1% yeast extract, 2% peptone, and 2% glucose. The YPD dishes were incubated at 37 °C for 24 h. The cells were washed with deionized (DI) water three times by centrifugation, then they were suspended in sterilized DI water at various dilutions (1:10). The cells were incubated on agar plates at 37 °C for 24 h for determination of the number of cells. The diameter of yeast cells varied from 4 μm to 7 μm . The number of cells was 1.3×10^9 colony forming units per milliliter (cfu/mL). The conductivity of DI water is 6 mS/m.

3.2. Device Fabrication

The microfluidic device was fabricated by a photolithography technique. First, the masks were designed by layout editor software (LayoutEditor, 2014, Juspertor GmbH, Unterhaching, Germany). Two masks (top and bottom) were written by a laser lithography system (μPG501 , Heidelberg Instruments, Heidelberg, Germany) on the chromium (Cr) masks. Firstly, the top layer mold was fabricated by two-step photolithography using SU-8 2025 negative photoresist (MicroChem, Newton, MA, USA). The first layer had a thickness of 25 μm and was spin-coated onto a silicon substrate.

After pre-baking, the first layer photoresist was exposed to top layer Cr mask by using a mask aligner (Suss MicroTech MA-6, SÜSS MicroTec AG, Garching, Germany) and post-baking with development. Then, the second layer with 60 μm thickness was spin-coated on the first photoresist layer and pre-baked. The bottom layer Cr mask was aligned with the substrate of the first photoresist layer and exposed to UV light. The photoresist substrate was post-baked and developed to obtain a top mold master. Following the SU-8 microchannel photolithography step for the top mold master, the bottom mold master with 60 μm thickness was fabricated. PDMS was prepared by thoroughly mixing PDMS pre-polymers (SYLGARD184A, Dow Corning Silicones Malaysia Sdn Bhd, Selangor, Malaysia) with curing agents (SYLGARD 184B, Dow Corning Silicones Malaysia Sdn Bhd, Selangor, Malaysia) in a ratio of 10:1 by weight and poured on an SU-8 mold master (top and bottom mold master). A PDMS microchannel was obtained after curing overnight at room temperature. The top side PDMS and bottom side PDMS were cleaned with isopropyl alcohol and treated by oxygen plasma (Plasma Etch PE-25, Plasma Etch, Inc., Carson City, NV, USA) for 25 seconds to increase bonding strength. The alignment of both side PDMS channels was completed in less than two minutes to prevent loss of oxygen plasma effectiveness. Finally, the right and left sides of the microchannel chip were cut, leaving a square (60 $\mu\text{m} \times 120 \mu\text{m}$) hole for insertion of a microneedle. A commercially-available tungsten needle (SE-20TB, Signatone, Gilroy, CA, USA) coated by parylene was utilized as a measuring electrode (two microneedles). The tip diameter, shank diameter, and length of tungsten needle are 20 μm , 250 μm , and 31.7 mm, respectively.

3.3. Experimental Setup

The microchannel chip system was placed under a microscope (Olympus Inverted Microscopes IX71, Olympus Corporation, Tokyo, Japan) to monitor the sensing area. Two microneedles held by the micromanipulator (EB-700, Everbeing, St. Hsinchu, Taiwan) were inserted into microchannel chip through the square hole at right and left side of the chip. The gap between microneedles was fixed at 20 μm for this experiment. A schematic of the experimental setup is shown in Figure 2. The impedance analyzer (Hioki IM3570, Shanghai, China) was connected with two microneedles as an input, and was displayed on the computer. The sample of the solution and yeast concentration was introduced using 3 mL syringes controlled by syringe pumps (KDS LEGATO 111, KD Scientific, Holliston, MA, USA). Two flexible tygon tubes (Tygon Microbore tubing, Cole-Parmer, Vernon Hills, IL, USA) connected to the syringes and waste bottle were inserted into the PDMS layer at the inlets for the introduction of liquids and outlet of waste liquids.

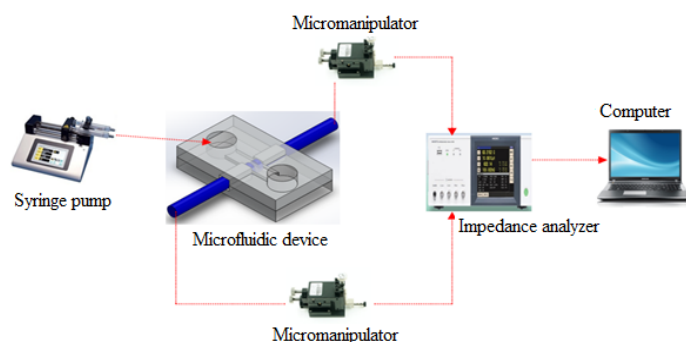


Figure 2. A schematic diagram of the experimental set-up.

3.4. Electrical Measurement Procedure

Initially, 1 mL of each of the four different solution samples (DI water and phosphate-buffered saline (PBS) with three concentrations: 300 mOsm, 1500 mOsm, and 3000 mOsm) was prepared for the chip characterization measurement. Each sample was loaded into a syringe, and five measurement cycles were conducted to measure all samples. The sample was driven through the microchannel using

a syringe pump with the flow rate of the syringe pump kept constant (60 $\mu\text{L}/\text{min}$). The microneedles connected to impedance analyzer were used to measure the impedance of each solution. Impedance spectra (impedance and phase vs. frequency) were measured using an AC signal frequency range from 100 Hz to 1 MHz with an applied voltage of 1 Volt to differentiate variations of solution samples. Between each PBS sample measurement, the microchannel chip was flushed by DI water for 3 min. The data were recorded with the impedance analyzer GUI (graphical user interface) software (v3.10, Hioki E.E. Corporation, Nagano, Japan) and post-processed in MATLAB (R2011, MathWorks Inc., Natick, MA, USA).

Meanwhile, for yeast cell concentration detection measurement, 1 mL of each of seven different concentrations of sample from 10^2 to 10^9 cfu/mL was prepared for the measurement. The sample was driven through the microchannel at a flow rate of 6 $\mu\text{L}/\text{min}$. An AC signal frequency range from 100 kHz to 5 MHz with an applied voltage of 1 Volt was utilized for cell concentration detection measurement. The impedance change during the passage of yeast cells at the sensing area was measured. Impedance at three frequencies (100 kHz, 500 kHz, and 1 MHz) was measured to observe the changing of impedance for each sample.

In order to perform the measurement, the impedance analyzer was self-calibrated by using short and open standard calibration. Furthermore, to calibrate the chip, impedance of $1 \times \text{PBS}$ (1 time the physiologic concentration of 300 mOsm) solution was measured at the 20 μm electrode gap. All experiments were conducted at room temperature, and three microfluidic devices were utilized for reproducibility testing on the device. To validate the equivalent circuit model, impedance of the medium between microneedle was measured. Two separate solutions with different conductivities were used. The solutions were sterilized DI water and PBS (phosphate-buffered saline) with conductivities 6 mS/m and 1.4 S/m, respectively.

4. Results and Discussion

As a proof of concept, we studied the dependency of the impedance on various concentrations of cells in the suspension medium by using this microfluidic device. Figure 3 presents the measured impedance spectra and fitting spectra (on a log scale) of the system for two of microchannels filled with sterilized DI water and PBS at frequency range 1 kHz to 1 MHz. For simulation, 100 data points on the impedance-measured spectrum were used as input to the equivalent circuit (see Figure 1b) and the fitting impedance spectrum was generated using MATLAB. For high-conductivity fluid (PBS), the results show two domains—an electrical double layer (EDL) region and a resistive region [24]. The EDL occurred in the low frequency range from 1 kHz to approximately 300 kHz, whereas the resistive region occurred in high frequency from 300 kHz to 1 MHz. The agreement between the measured and fitting spectra results indicated that our developed circuit model for this system is able to determine the impedance characteristics of solution medium. Figure 4 shows the impedance spectrum measurement of one device when filled with DI water and three different concentrations of PBS solution. Individual curves are the average of five frequency sweeps. Resulting IFC data reflect properties of both the current path around the sample and the material sample in the microchannel (i.e., dielectric properties of the microdevice) [25]. The results show that the sensor can differentiate between solution media due to the change in relative dielectric permittivity of the solution. A rising of the solution conductivity affected the capacitance measurement as the result of an increase in capacitance and thus a decrease in the impedance measured [26].

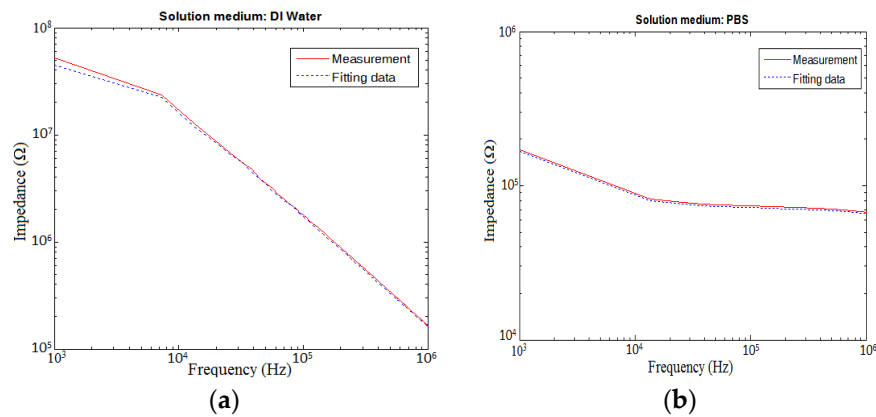


Figure 3. Impedance spectra of sample solution together with their fitting spectra (a) deionized (DI) water; (b) phosphate-buffered saline (PBS).

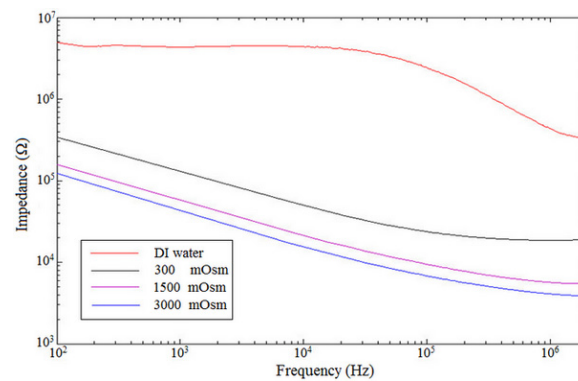


Figure 4. Impedance spectra of DI water and varying concentrations of PBS measured by impedance flow cytometry (IFC).

Yeast cells at different concentrations were utilized to illustrate the cell detection capability of the device. Yeast cell concentrations ranging from 10^2 to 10^9 cfu/mL were infused inside the microchannel with a fixed flow rate $6 \mu\text{L}/\text{min}$. As can be seen in Figure 5, the yeast cells were flown passes through the microneedles, which have fixed gap ($20 \mu\text{m}$). A sweep frequency (100 kHz to 5 MHz) AC signal (1 Volt) was applied to one side of the microneedle, and the current entering at another side of the microneedle was measured to calculate the impedance of that concentration of yeast cells in DI water. Initially, 10^9 cfu/mL were injected, resulting in a drop in impedance by referring to the impedance of DI water as a control. Afterward, the microchannel chip was washed by PBS followed by DI water at maximum flow rate.

The maximum flow rate that liquid can flow inside microchannel without leaking is $300 \mu\text{L}/\text{min}$. Figure 6a shows the impedance spectra of yeast cell in DI water with different cell concentrations in the range 10^4 to 10^9 cfu/mL, along with DI water as a reference. After washing the microchannel, 10^8 cfu/mL was infused to the microchannel, resulting in an increase in impedance. It can be seen that the impedance spectra of yeast cells in DI water across the sensing area (two microneedles) increase with decreasing cell concentration [14]. According to the observation, it can be said that cell suspensions with high concentration are more conductive than those with lower concentrations. The conductivity of a solution varies proportionally to the cell concentration at a fixed volume of solution [27]. In some studies, the relative dielectric permittivity and charged polyelectrolytes inside the cell may also affect the impedance of solution [14]. The optimum region for the sensing microneedle to differentiate the cell concentration in DI water is between 500 kHz to 5 MHz. The impedance values

of the suspensions in this frequency region were significantly different from each other. The experiment was repeated two times, and showed similar results.

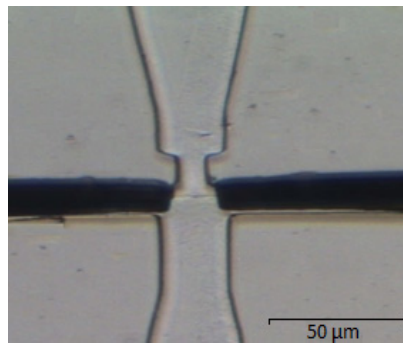


Figure 5. Image of the sensing area of the device.

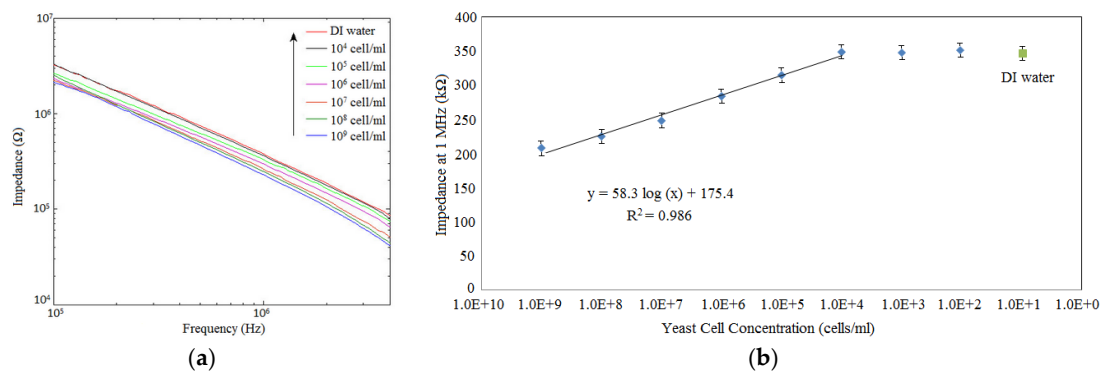


Figure 6. (a) Impedance spectra of yeast cells in water with cell concentrations ranging from 10² to 10⁹ cfu/mL, along with DI water as control; (b) The linear relationship between the logarithmic value of the concentration of yeast cells and the impedance measured at 1 MHz. Error bars are standard deviations of 5 measurements.

In cell detection experiment, we did not perform the measurement at frequency lower than 100 kHz, since the EDL will influence the measurement at low frequencies (approximately below 300 kHz) [12,17]. In order to investigate the relationship between impedance value and cell concentration, we selected 1 MHz as the best representative frequency. Figure 6b illustrates the impedance responses of the sample containing different yeast cell concentrations and DI water at frequency measurement 1 MHz. The impedance of the solution was significantly increased from 207.63 kΩ to 225.42 kΩ, 247.61 kΩ, 284.48 kΩ, 314.64 kΩ, and 348.51 kΩ when the yeast concentration decreased from 10⁹ cfu/mL to 10⁸ cfu/mL, 10⁷ cfu/mL, 10⁶ cfu/mL, 10⁵ cfu/mL, and 10⁴ cfu/mL, respectively. After the cell concentrations were lower than 10⁴ cfu/mL, impedance values showed no significant changes between each other or DI water. In addition, the pattern of the result shows a linear relationship between the impedance and the logarithmic value of the cell concentration at cell concentrations from 10⁴ cfu/mL to 10⁹ cfu/mL (see Figure 6b). The linear regression equation of this result is $Z \text{ (k}\Omega\text{)} = 58.3 \log C \text{ (cells/mL)} + 175.4$ (Where Z —Impedance and C —Cell concentration), with $R^2 = 0.986$. The detection limit was calculated to be 1.2×10^4 cfu/mL. Error bars are standard deviations of five measurement cycles. Based on this linear regression equation, the impedance of the yeast suspensions can be used to estimate the cell concentration in DI water suspensions. This device can be utilized to quantify cells in suspensions other than impedance microbiology and impedance biosensors for bacteria detection, since the detection limit of this method is comparable with other sensors. The reported sensor for detection of pathogenic bacteria are quartz crystal microbalance (QCM) immunosensors for detection of *Salmonella* with detection limits of

9.9×10^5 cfu/mL [28], surface plasmon resonance (SPR) sensor for the detection of *E. coli* O157:H7 with a detection limit of 10^7 cfu/mL [29] and SPR immunosensors for the detection of *Salmonella enteritidis* and *Listeria monocytogenes* with detection limits of 10^6 cfu/mL [30].

As the result, we conclude that this device was capable of detecting the cell concentrations in solution medium at the high frequency range between 100 kHz and 5 MHz. In this experiment, we did not determine the detection capability at frequencies lower than 100 kHz. For future work, we will focus on the size and shape of microneedle [31–33], single cell detection [34], and will utilize non-polarizable electrodes (i.e., Ag/AgCl—to eliminate the EDL) in order to improve the performance of the device.

5. Conclusions

In summary, we demonstrated a very simple, label-free, and low-cost microfluidic device for solution detection and cell concentration detection in a suspension medium. This device contains reusable microneedles which can be inserted into a disposable PDMS microchannel. We found that the impedance value decreased with the increase of cell concentration in the solution medium. The capability of this device to differentiate the concentration of cells from 10^9 cfu/mL to 10^4 cfu/mL shows the core functionality of the proposed sensor, even though the manufacturing cost was significantly lower. As a proof of concept, yeast cells were used in this study, and we emphasize that this sensing technique can be applied to a variety of cell types with diameter size in a range from 5 μ m to 25 μ m. It is recommended that only one measurement cycle be performed for each PDMS microchip, in order to avoid the potential spread of contamination to samples. The device is suitable for early cancer cell detection and water contamination application in developing countries, since it significantly reduces the fabrication cost ($\approx 30\%$ fabrication cost was reduced based on facility rental and raw material usage).

Acknowledgments: The research was supported by the Ministry of Higher Education of Malaysia (Grant Nos. 4L640 and 4F351), and Universiti Teknologi Malaysia (Grant Nos. 03E11, 03G47, 4J148, 02G46, 03H82 and 03H80); we thank them for funding this project and for their endless support

Author Contributions: Muhammad Asraf Mansor, designed and performed the experiments and Mohd Ridzuan Ahmad supervised the project and edited the article. Masaru Takeuchi, Masahiro Nakajima, and Yasuhisa Hasegawa contributed to the advices, reagents, materials and microchip fabrication facilities.

Conflicts of Interest: The authors declare no conflict of interest.

References

1. Kantara, C.; O'Connell, M.R.; Luthra, G.; Gajjar, A.; Sarkar, S.; Ullrich, R.L.; Singh, P. Methods for detecting circulating cancer stem cells (CCSCs) as a novel approach for diagnosis of colon cancer relapse/metastasis. *Lab. Investig.* **2015**, *95*, 100–112. [[CrossRef](#)] [[PubMed](#)]
2. Ciceron, L.; Jaureguierry, G.; Gay, F.; Danis, M. Development of a Plasmodium PCR for monitoring efficacy of antimalarial treatment. *J. Clin. Microbiol.* **1999**, *37*, 35–38. [[PubMed](#)]
3. Pandey, P.K.; Kass, P.H.; Soupir, M.L.; Biswas, S.; Singh, V.P. Contamination of water resources by pathogenic bacteria. *AMB Express* **2014**, *4*, 51. [[CrossRef](#)] [[PubMed](#)]
4. Coulter, W.H. High speed automatic blood cell counter and cell analyzer. *Proc. Natl. Electron. Conf.* **1956**, *12*, 1034–1040.
5. Saleh, O.A.; Sohn, L.L. Quantitative sensing of nanoscale colloids using a microchip Coulter counter. *Rev. Sci. Instrum.* **2001**, *72*, 4449. [[CrossRef](#)]
6. Khaw, B.; Scott, J.; Fallon, J.; Cahill, S.; Haber, E.; Homcy, C. Myocardial injury: Quantitation by cell sorting initiated with antimyosin fluorescent spheres. *Science* **1982**, *217*, 1050–1053. [[CrossRef](#)]
7. Holmes, D.; Morgan, H. Single cell impedance cytometry for identification and counting of CD4 T-cells in human blood using impedance labels. *Anal. Chem.* **2010**, *82*, 1455–1461. [[CrossRef](#)] [[PubMed](#)]
8. Gou, H.-L.; Zhang, X.-B.; Bao, N.; Xu, J.-J.; Xia, X.-H.; Chen, H.-Y. Label-free electrical discrimination of cells at normal, apoptotic and necrotic status with a microfluidic device. *J. Chromatogr. A* **2011**, *1218*, 5725–5729. [[CrossRef](#)] [[PubMed](#)]

9. Du, E.; Ha, S.; Diez-Silva, M.; Dao, M.; Suresh, S.; Chandrakasan, A.P. Electric impedance microflow cytometry for characterization of cell disease states. *Lab Chip* **2013**, *13*, 3903–3909. [[CrossRef](#)] [[PubMed](#)]
10. Liu, Y.-S.; Banada, P.P.; Bhattacharya, S.; Bhunia, A.K.; Bashir, R. Electrical characterization of DNA molecules in solution using impedance measurements. *Appl. Phys. Lett.* **2008**, *92*, 143902. [[CrossRef](#)]
11. Javanmard, M.; Talasaz, A.H.; Nemat-Gorgani, M.; Pease, F.; Ronaghi, M.; Davis, R.W. Targeted cell detection based on microchannel gating. *Biomicrofluidics* **2007**, *1*, 044103. [[CrossRef](#)] [[PubMed](#)]
12. Segerink, L.I.; Sprenkels, A.J.; ter Braak, P.M.; Vermes, I.; van den Berg, A. On-chip determination of spermatozoa concentration using electrical impedance measurements. *Lab Chip* **2010**, *10*, 1018–1024. [[CrossRef](#)] [[PubMed](#)]
13. Gawad, S.; Schild, L.; Renaud, P.H. Micromachined impedance spectroscopy flow cytometer for cell analysis and particle sizing. *Lab Chip* **2001**, *1*, 76–82. [[CrossRef](#)] [[PubMed](#)]
14. Esfandyarpour, R.; Javanmard, M.; Koochak, Z.; Harris, J.S.; Davis, R.W. Nanoelectronic impedance detection of target cells. *Biotechnol. Bioeng.* **2014**, *111*, 1161–1169. [[CrossRef](#)] [[PubMed](#)]
15. Wang, J.; Chatrathi, M.P.; Mulchandani, A.; Chen, W. Capillary electrophoresis microchips for separation and detection of organophosphate nerve agents. *Anal. Chem.* **2001**, *73*, 1804–1808. [[CrossRef](#)] [[PubMed](#)]
16. Park, K.; Suk, H.-J.; Akin, D.; Bashir, R. Dielectrophoresis-based cell manipulation using electrodes on a reusable printed circuit board. *Lab Chip* **2009**, *9*, 2224–2229. [[CrossRef](#)] [[PubMed](#)]
17. Emaminejad, S.; Javanmard, M.; Dutton, R.W.; Davis, R.W. Microfluidic diagnostic tool for the developing world: Contactless impedance flow cytometry. *Lab Chip* **2012**, *12*, 4499–4507. [[CrossRef](#)] [[PubMed](#)]
18. Emaminejad, S.; Paik, K.; Tabard-Cossa, V.; Javanmard, M. Portable cytometry using microscale electronic sensing. *Sens. Actuators B Chem.* **2016**, *224*, 275–281. [[CrossRef](#)] [[PubMed](#)]
19. Sun, T.; Morgan, H. Single-cell microfluidic impedance cytometry: A review. *Microfluid. Nanofluid.* **2010**, *8*, 423–443. [[CrossRef](#)]
20. Mansor, M.A.; Ahmad, M.R. Single Cell Electrical Characterization Techniques. *Int. J. Mol. Sci.* **2015**, *16*, 12686–12712. [[CrossRef](#)] [[PubMed](#)]
21. Mansor, M.A.; Ahmad, M.R. A Simulation Study of Single Cell Inside an Integrated Dual Nanoneedle-Microfluidic System. *J. Teknol.* **2016**, *78*, 59–65.
22. Foster, K.R.; Schwan, H.P. Dielectric properties of tissues and biological materials: A critical review. *Crit. Rev. Biomed. Eng.* **1989**, *17*, 25–104. [[PubMed](#)]
23. Jang, L.-S.; Wang, M.-H. Microfluidic device for cell capture and impedance measurement. *Biomed. Microdevices* **2007**, *9*, 737–943. [[CrossRef](#)] [[PubMed](#)]
24. Morgan, H.; Sun, T.; Holmes, D.; Gawad, S.; Green, N.G. Single cell dielectric spectroscopy. *J. Phys. D Appl. Phys.* **2007**, *40*, 61–70. [[CrossRef](#)]
25. Ayliffe, H.E.; Frazier, A.B.; Rabbitt, R.D. Electric impedance spectroscopy using microchannels with integrated metal electrodes. *J. Microelectromech. Syst.* **1999**, *8*, 50–57. [[CrossRef](#)]
26. Heidari, M.; Azimi, P. Conductivity effect on the capacitance measurement of a parallel-plate capacitive sensor system. *Res. J. Appl. Sci. Eng. Technol.* **2011**, *3*, 53–60.
27. Yang, L. Electrical impedance spectroscopy for detection of bacterial cells in suspensions using interdigitated microelectrodes. *Talanta* **2008**, *74*, 1621–1629. [[CrossRef](#)] [[PubMed](#)]
28. Park, I.S.; Kim, W.Y.; Kim, N. Operational characteristics of an antibody-immobilized QCM system detecting *Salmonella* spp. *Biosens. Bioelectron.* **2000**, *15*, 167–172. [[CrossRef](#)]
29. Fratamico, P.M.; Strobaugh, T.P.; Medina, M.B.; Gehring, A.G. Detection of *Escherichia coli* 0157:H7 using a surface plasmon resonance biosensor. *Biotechnol. Tech.* **1998**, *12*, 571–576. [[CrossRef](#)]
30. Koubová, V.; Brynda, E.; Karasová, L.; Škvor, J.; Homola, J.; Dostálek, J.; Tobiška, P.; Rošický, J. Detection of foodborne pathogens using surface plasmon resonance biosensors. *Sens. Actuators B Chem.* **2001**, *74*, 100–105. [[CrossRef](#)]
31. Ahmad, M.R.; Nakajima, M.; Kojima, S.; Homma, M.; Fukuda, T. Buckling nanoneedle for characterizing single cells mechanics inside environmental SEM. *IEEE Trans. Nanotechnol.* **2011**, *10*, 226–236. [[CrossRef](#)]
32. Shen, Y.; Nakajima, M.; Ridzuan Ahmad, M.; Kojima, S.; Homma, M.; Fukuda, T. Effect of ambient humidity on the strength of the adhesion force of single yeast cell inside environmental-SEM. *Ultramicroscopy* **2011**, *111*, 1176–1183. [[CrossRef](#)] [[PubMed](#)]

33. Ahmad, M.R.; Nakajima, M.; Kojima, S.; Homma, M.; Fukuda, T. Mechanical properties characterization of individual yeast cells using environment-SEM nanomanipulation system. In Proceedings of the International Conference on Intelligent Robots and Systems-IROS, San Diego, CA, USA, 29 October–2 November, 2007; pp. 596–601.
34. Ahmad, M.R.; Nakajima, M. Single Cells Electrical Characterizations using Nanoprobe via ESEM-Nanomanipulator System. In Proceedings of the 2009 9th IEEE Conference on Nanotechnology (IEEE-NANO), Genoa, Italy, 26–30 July 2009.



© 2017 by the authors; licensee MDPI, Basel, Switzerland. This article is an open access article distributed under the terms and conditions of the Creative Commons Attribution (CC BY) license (<http://creativecommons.org/licenses/by/4.0/>).